

# Rat model of spinal cord injury preserving dura mater integrity and allowing measurements of cerebrospinal fluid pressure and spinal cord blood flow

Marc Soubeyrand · Elisabeth Laemmel ·  
Charles Court · Arnaud Dubory · Eric Vicaut ·  
Jacques Duranteau

Received: 26 September 2012/Revised: 25 February 2013/Accepted: 5 March 2013/Published online: 19 March 2013  
© Springer-Verlag Berlin Heidelberg 2013

## Abstract

**Purposes** Cerebrospinal fluid (CSF) pressure elevation may worsen spinal cord ischaemia after spinal cord injury (SCI). We developed a rat model to investigate relationships between CSF pressure and spinal cord blood flow (SCBF).

**Methods** Male Wistar rats had SCI induced at Th10 ( $n = 7$ ) or a sham operation ( $n = 10$ ). SCBF was measured using laser-Doppler and CSF pressure via a sacral catheter. Dural integrity was assessed using subdural methylene-blue injection ( $n = 5$ ) and myelography ( $n = 5$ ).

**Results** The SCI group had significantly lower SCBF ( $p < 0.0001$ ) and higher CSF pressure ( $p < 0.0001$ ) values compared to the sham-operated group. Sixty minutes after SCI or sham operation, CSF pressure was  $8.6 \pm 0.4$  mmHg in the SCI group versus  $5.5 \pm 0.5$  mmHg in the sham-operated group. No dural tears were found after SCI.

**Conclusion** Our rat model allows SCBF and CSF pressure measurements after induced SCI. After SCI, CSF pressure significantly increases.

**Keywords** Spinal cord injury · Regional blood flow · Spinal cord blood flow · Cerebrospinal fluid pressure · Ischaemia

## Introduction

Spinal cord injury (SCI) compromises the conduction of sensory and motor impulses between the encephalon and the peripheral nervous system, causing motor, sensory, and autonomous impairments below the level of lesion, for which no treatments have been proven effective [1].

In SCI, the initial parenchymal damage caused directly by the trauma is the primary injury, which is followed by a number of biological events, known as the secondary injury and responsible for an increase in lesion size [2, 3]. Among these events, ischaemia plays a crucial role [4, 5].

The spinal cord is surrounded by cerebrospinal fluid (CSF) contained within the subdural space. When the pressure of the CSF exceeds a critical threshold, a tamponade effect occurs, decreasing the flow of blood and causing spinal cord ischaemia [6]. Conversely, drainage to

E. Vicaut and J. Duranteau have similarly contributed to the study.

M. Soubeyrand · E. Laemmel · A. Dubory · E. Vicaut ·  
J. Duranteau  
Equipe universitaire 3509 Paris VII-Paris XI-Paris XIII,  
Microcirculation, Bioénergétique, Inflammation et Insuffisance  
circulatoire aiguë, Paris Diderot-Paris VII University,  
Paris, France  
e-mail: elisabeth.laemmel@univ-paris-diderot.fr

A. Dubory  
e-mail: arnauldubory@hotmail.fr

E. Vicaut  
e-mail: eric.vicaut@univ-paris-diderot.fr

J. Duranteau  
e-mail: jduranteau@me.com

M. Soubeyrand (✉) · C. Court · A. Dubory  
Service de Chirurgie Orthopédique, Hôpital de Bicêtre,  
CHU Bicêtre, Hôpitaux universitaires Paris-Sud, Assistance  
Publique—Hôpitaux de Paris, 78 Rue Général Leclerc,  
94270 Le Kremlin-Bicêtre, France  
e-mail: soubeyrand.marc@wanadoo.fr

C. Court  
e-mail: charles.court@bct.aphp.fr

J. Duranteau  
Service d'Anesthésie Réanimation, Hôpital de Bicêtre,  
CHU Bicêtre, Hôpitaux universitaires Paris-Sud, Assistance  
Publique—Hôpitaux de Paris, 78 Rue Général Leclerc,  
Le Kremlin-Bicêtre, France

restore normal CSF pressure can improve spinal cord blood flow (SCBF), as demonstrated in human patients during aortic cross clamping for aortic aneurysm surgery [7–9].

In a study of 22 patients with SCI, Kwon et al. [10] found that CSF pressure increased during the decompressive surgery (peak of  $21.7 \pm 1.5$  mmHg) and continued to increase afterwards in the postoperative period (peak of  $30.6 \pm 2.3$  mmHg), thereby exceeding the physiological values. An intact dura mater allowing a CSF pressure increase may be the rule after SCI, as a study of 258 surgical patients with spinal fractures found dural tears in only 20 (7.7 %) patients [11].

If CSF pressure elevation after SCI worsens the spinal cord ischaemia, then CSF drainage may hold potential for decreasing the final lesion size, thereby improving neurological outcomes. An experimental SCI model allowing simultaneous monitoring of CSF pressure and SCBF would be a valuable tool for investigating the relationships between these two variables. Several models for assessing the effect of SCI on SCBF have been described [12–15]. Other models characterised by a decrease in the blood supply to the spinal cord have been developed to investigate relationships between SCBF and CSF pressure, but do not involve traumatic SCI [16–18]. Most of the models developed for assessing CSF pressure rely on large animals such as dogs and pigs, whereas rats are the most widely used animals to investigate SCI [19]. The only small-animal SCI model designed to allow both CSF pressure and SCBF measurements is a rabbit model that does not include an evaluation of dural integrity after SCI; in addition, the absence in this model of baseline (pre-SCI) CSF pressure measurement precludes an evaluation of SCI effects on CSF pressure [20].

The objective of the present study was twofold: to determine whether experimental weight-dropping SCI can be induced in a rat model without compromising dural integrity and to develop a protocol for simultaneously measuring CSF pressure and SCBF after induced SCI.

## Materials and methods

All methodologies used in this experimental animal study were approved by the bioethics committee of the Lariboisière School of Medicine (CEEALV/2011-08-01). The animals were kept in individual quarters in a room with a 12-h light/dark cycle and free access to food and water.

In the first part of the study, we have used 20 animals to measure SCBF and CSF pressure. In the second part of the study, ten other animals were used to assess the integrity of the dura after SCI.

## Part 1: Surgical preparation and measurements of CSF pressure and SCBF

A total of 20 male Wistar rats weighing 370–420 g were used. In ten animals, an experimental SCI was performed (SCI group), while ten other animals underwent a simple laminectomy without SCI (sham-operated group).

Thirty minutes after a subcutaneous buprenorphine injection (0.05 mg/kg), intraperitoneal (IP) sodium pentobarbital (60 mg/kg) was given for anaesthesia. To maintain body temperature between 37 and 38 °C, the animal was placed on a heating blanket connected to a rectal thermometer. A tracheotomy was performed to permit ventilation with room air. A cannula inserted into the left carotid artery was connected to a Truwave Pressure Transducer PX600 (Edward Lifesciences®, Irvine, CA, USA) to monitor mean arterial blood pressure (MABP). This transducer had a measurement range of –50 (vacuum) to 300 mmHg, a sensitivity of  $5 \mu\text{V}/\text{V}/\text{mmHg} \pm 1\%$  ( $\pm 0.4$  mmHg), a non-linearity and hysteresis of  $\pm 1.5\%$  of reading or  $\pm 1$  mmHg and a natural frequency  $>200$  Hz. MABP signals were digitized at 5 kHz and transferred to a Biopac MP30 physiological data-acquisition system (Biopac Systems, Goletta, CA, USA). The latter was connected to a personal computer (Microsoft XP, Microsoft, Redmont, WA, USA) on which the Student Lab Pro® software (Biopac Systems, Goletta, CA, USA) allowed continuous recording of the MABP. The carotid catheter was also used to provide continuous hydration with 0.9 % saline (10 mL/kg/h).

The rat was placed in the prone position, a midline incision was made, and laminectomy was performed from the ninth (Th9) to the eleventh (Th11) thoracic vertebra to expose the dura mater surrounding the spinal cord. A second laminectomy was performed from the first to the third sacral vertebra (S1–S3) to expose the dura mater surrounding the cauda equina. Then, a 24-gauge catheter surrounding a 25-gauge needle was inserted through the dura mater into the subdural space (Fig. 1). Afterwards, the 25-gauge needle guiding the catheter was withdrawn while the catheter was carefully left in the subarachnoid space, taking care of avoiding CSF leakage. The lumen of the catheter was filled with saline to take off any air bubble. Biological glue composed of bovine serum albumin and glutaraldehyde (BioGlue®, Gamida, Eaubonne, France) was used to secure the catheter and to preclude CSF leakage around the catheter. The subdural catheter was connected to another Truwave Pressure Transducer PX600 (Edward Lifesciences®, Irvine, CA, USA) which technical features are described above. CSF pressure signals were acquired at a sampling rate of 5 kHz and transferred to the Biopac MP30 described above and also connected to the Student Lab Pro® software which allowed continuous recording of the CSF pressure. After catheter insertion,

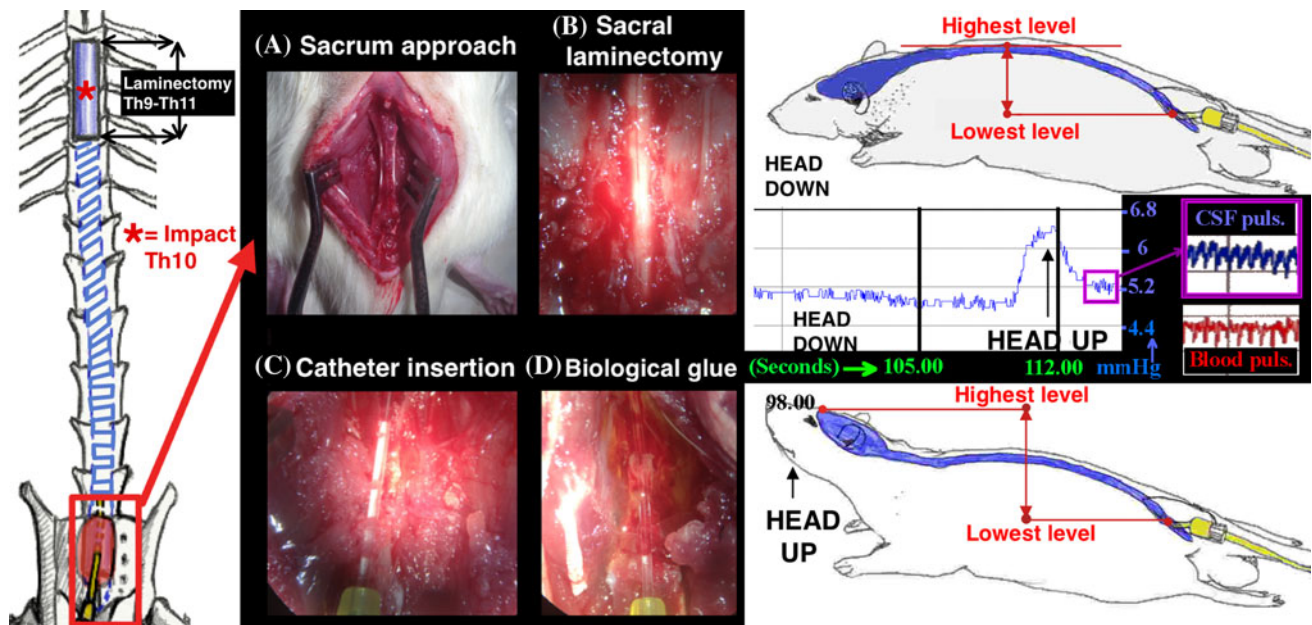


**Fig. 1** *Left panel:* the SCI was induced at the Th10 level and the subarachnoid catheter was inserted at the sacrum level *Middle panel* Technique for subarachnoid catheter insertion. The sacrum was first approached through a dorsal midline incision (a) and laminectomy was then performed to expose the dural sheath surrounding the cauda equina (b). A 24-gauge catheter was inserted through the dura mater (c). Cerebrospinal fluid (CSF) reflux into the catheter is usually visible. A layer of biological glue was applied to prevent CSF leaks

around the catheter (d). *Right panel:* To ascertain correct catheter position within the subdural space, a head-up test was performed. The test was considered positive when elevation of the animal's head induced a CSF pressure peak by increasing the height difference between the highest (skull) and lowest (sacrum) points of the dural compartment. Presence of CSF pressure pulsation ("CSF puls.") synchronous with arterial blood pulsations ("Blood puls.") was another indicator of correct position in the subdural space

we routinely checked that the head-up test was positive, confirming proper catheter position within the subdural space (Fig. 1). The test was considered positive when each head elevation induced a CSF pressure elevation at the sacral level. Moreover, after positioning the sacral catheter, the visualisation of CSF pressure pulsations was considered an indicator of proper positioning in the subarachnoid space.

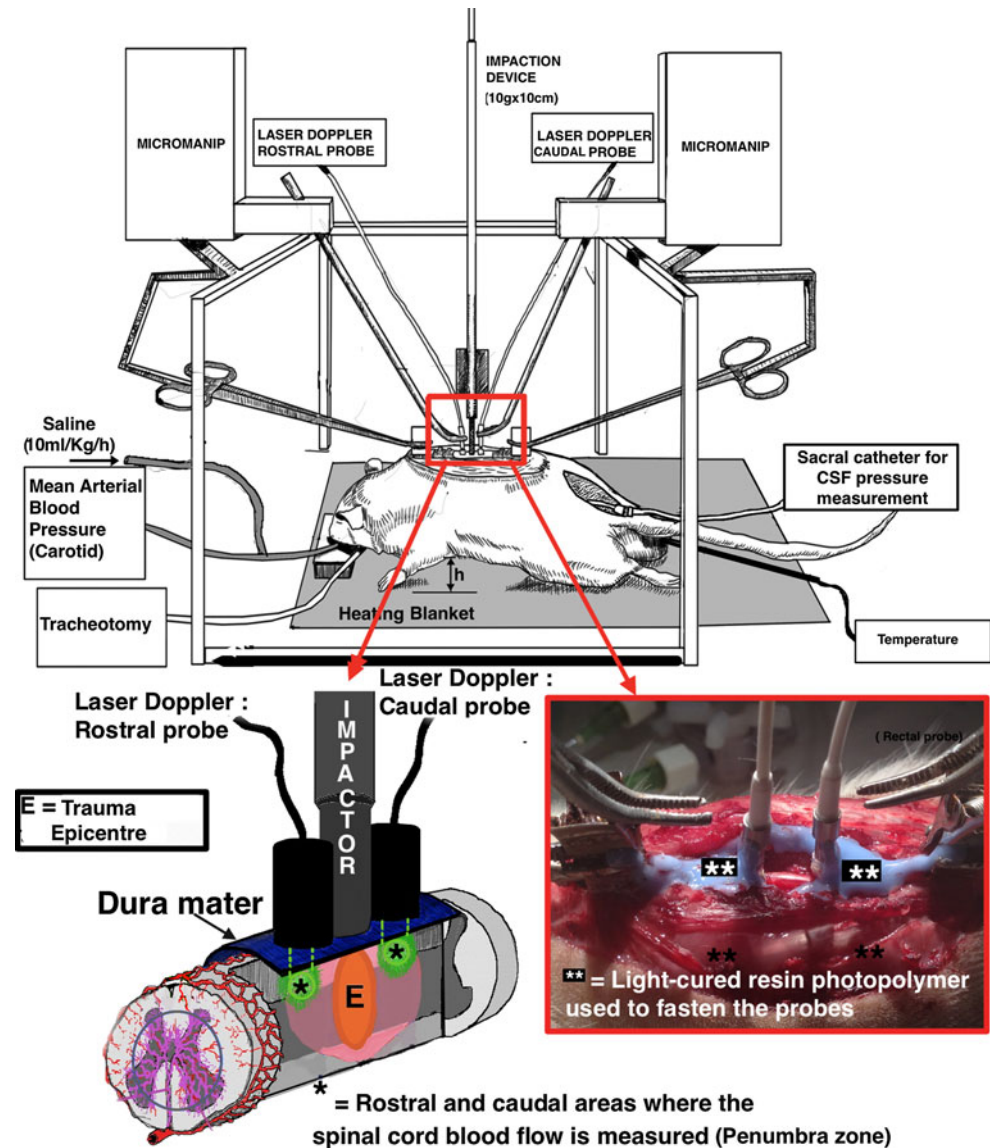
A stereotaxic frame was clamped to the spinous processes of Th7 and Th13 with the thorax elevated from the heating blanket to eliminate any influence of respiratory movements on spine position (Fig. 2). SCBF was measured using the laser-Doppler technique. This technique uses a monochromatic laser beam that penetrates the cord parenchyma and is reflected by the erythrocytes. The same probe that emits the beam receives the reflected part of the beam. Two probes (Probe 407 Small Straight Probe with Miniholders, Wavelength 780 nm, Perimed<sup>®</sup>, Lyon, France) were placed at a distance of 4 mm from the trauma epicentre, one rostrally and the other caudally, for SCBF measurement in the ischaemic penumbra zone surrounding the epicenter [4, 21] (Fig. 2). The distance between the epicenter and the center of each probe was 4 mm. A micromanipulator was used to position the probes in contact with the dura mater. To avoid any spinal cord displacements that might affect laser-Doppler measurements,

the probes were secured to the transverse processes of the underlying vertebrae using light-cured photopolymer resin (Opaldam<sup>®</sup>, Ultradent, South Jordan, UT, USA). The data were recorded continuously using Student Lab Pro<sup>®</sup> software (Biopac Systems).

For each time points and for each parameter (SCBF, MABP, CSF pressure), we used the Student Lab Pro<sup>®</sup> software (Biopac Systems, Goletta, CA, USA) to obtain the mean value of the period starting 30 s before the measurement point and finishing 30 s after. This value was recorded as the value of the corresponding time point.

At this point, no further manipulations were performed on the animal for 30 min, to allow stabilisation of the hemodynamic parameters. The end of this phase was defined as baseline. In one group of animals ( $n = 10$  animals), severe SCI was induced 5 min after baseline (defined as  $t_0$ ) using an apparatus which generated a trauma equivalent to the drop of a 10-g weight from a height of 10 cm on the cord at Th10. This apparatus was specifically designed in our own laboratory. The apparatus was composed of three pieces: a cylinder (the "tube") linkable to the stereotaxic frame, a cylindrical piece (the "impactor") used to transmit the impact to the spinal cord, a piece falling into the tube and delivering kinetic energy to the impactor. The impactor had a diameter of 3 mm, and had a flat tip that was polished to reduce the risk of inducing a

**Fig. 2** After surgical preparation, the rat is installed in a stereotaxic frame with the thorax elevated from the heating blanket. Micromanipulators (micromanip on the figure) are used to position two laser-Doppler probes in contact with the dura mater. The probes are then secured to the transverse processes of the underlying vertebrae using light-cured resin photopolymer. Spinal cord blood flow is measured rostrally and caudally to the epicentre, within the ischaemic penumbra zone



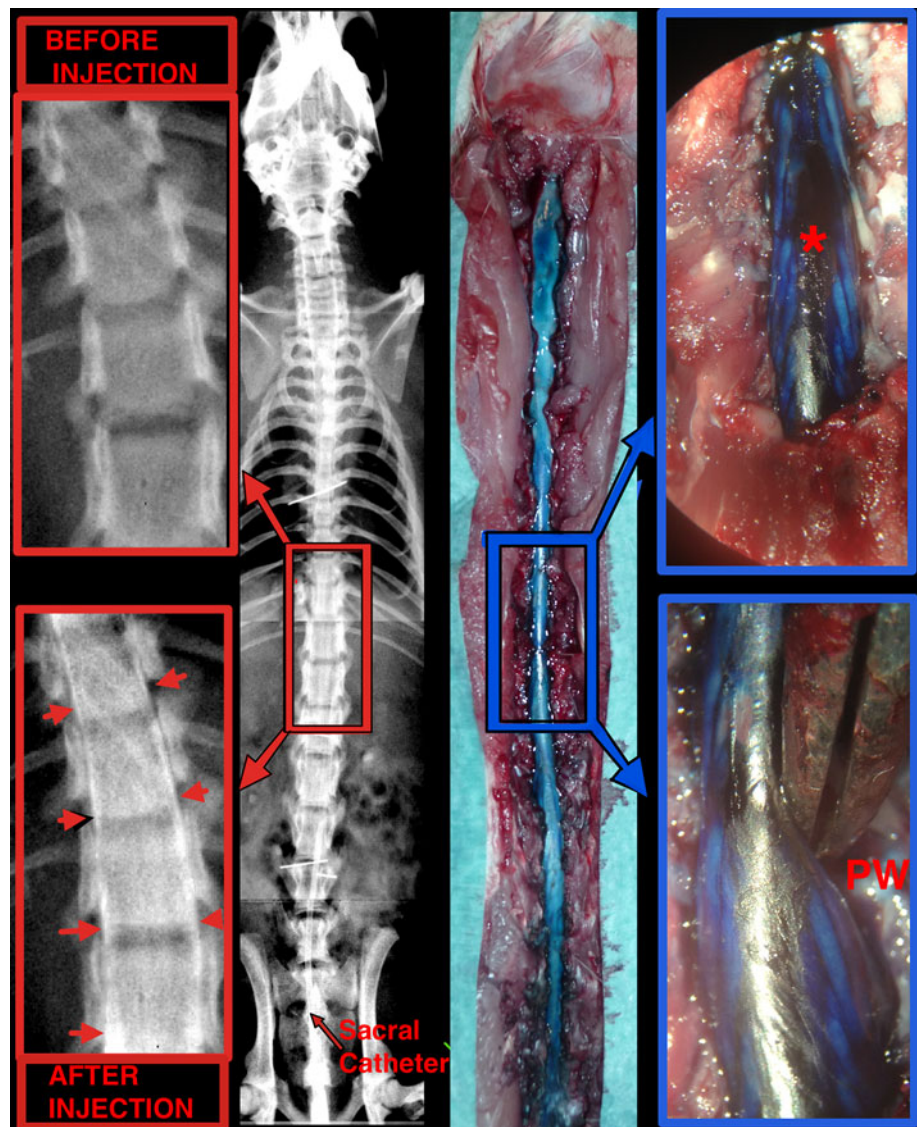
penetrating dural tear. A combination of passive magnets allowed to avoid multiple bounces of the impactor on the dura mater and, therefore, to ascertain the realisation of a unique impact on the spinal cord. The apparatus was recalibrated every ten impacts and the intensity of the impact remained constant through all the study. The reproducibility of the injury induced by the apparatus was previously assessed in another study by measuring the extent of the parenchymal haemorrhage with an ultrasound device [22]. Rostral and caudal SCBF, MABP, and CSF pressure were measured 5 ( $t_5$ ), 10 ( $t_{10}$ ), 15 ( $t_{15}$ ), 20 ( $t_{20}$ ), 30 ( $t_{30}$ ), 45 ( $t_{45}$ ), and 60 ( $t_{60}$ ) minutes after  $t_0$ . The experiment ended 60 min after  $t_0$  ( $t_{60}$ ), when each animal was euthanised with a lethal intravenous pentobarbital injection. Another group of animals ( $n = 10$  animals) underwent a sham operation. Inclusion of animals in each groups was determined at random. Predefined criteria for excluding

animals from the study were baseline MABP < 100 mmHg, death of the animal before  $t_{60}$ , and technical failure during SCI induction.

#### Part 2: Assessment of dural integrity

Ten rats were used specifically to assess the integrity of the dura mater 5 min after SCI (Fig. 3). Two techniques were used in different animals. Myelography was performed in five animals after SCI by injecting manually 100  $\mu$ l of a contrast agent (Amipaque<sup>®</sup>, Metrizamide 3.75 g/20 ml, Sanofi-Adventis, Paris, France) through the subdural catheter then obtaining anteroposterior and lateral radiographs of the entire spine with a Faxitron MX-20<sup>®</sup> (Faxitron, Licolnshire, IL, USA) which spatial resolution is 48  $\mu$ m (10 lp/mm). Each radiograph was examined for evidence of contrast-agent leakage, using Osirix<sup>®</sup> 3.8.1.

**Fig. 3** The integrity of the entire dura mater after the weight-dropping injury was assessed using two techniques: myelography after subdural contrast-agent injection and binocular inspection of the dural sac (*asterisk*) after subdural methylene-blue injection. Subdural injections were performed through the dural catheter. *PW* posterior wall of vertebra's body visualised by retracting the dural sac



software (Pixmeo, Geneva, Switzerland). In five other animals, 100  $\mu$ l of methylene blue was injected in the same manner after SCI. Then, the laminectomy was extended to the entire spine (C1 to S3) and the dura mater was inspected circumferentially using a binocular microscope to look for methylene-blue leakage.

#### Statistical analysis

Statistical analyses were performed using Statview<sup>®</sup> 5.0 software (SAS Institute, Cary, NC, USA). All results are reported as mean  $\pm$  SEM, with  $n$  being the number of animals.

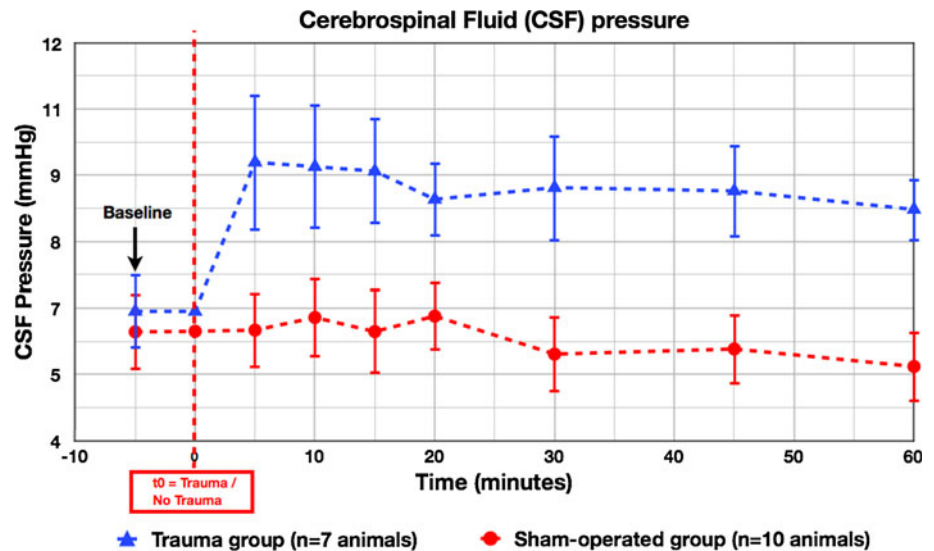
To assess the effect of SCI on CSF pressure and MABP, we performed two-way ANOVA (time and presence/absence of trauma). The effect of SCI on SCBF was evaluated by computing rostral and caudal SCBF values as

the percentages of baseline (rostral SCBF % and caudal SCBF %, respectively). Changes in rostral SCBF % and caudal SCBF % were analysed using three-way ANOVA (time, presence/absence of trauma, and rostral/caudal position relative to the epicentre). Post-hoc analyses were performed using the Bonferroni comparison test when ANOVA was significant. Values of  $p$  lower than 0.05 were considered significant.

#### Results

Three animals out of ten were excluded from the SCI group ( $n = 7$ ): two died before the end of the experiment, and in one animal the sacral catheter was accidentally withdrawn which has compromised the measurements. No animal was excluded from the sham-operated group ( $n = 10$ ).

**Fig. 4** Changes in cerebrospinal (CSF) pressure in the sham-operated and spinal cord injury (SCI) groups. During installation of the rat inside the stereotaxic frame, the thorax is elevated from the heating blanket, leading to an increase in CSF pressure measured with the sacral catheter (*asterisk*). Experimental SCI induced a significant increase in CSF pressure. The values shown correspond to mean  $\pm$  SEM



### Cerebrospinal fluid pressure

During insertion of the sacral catheter, no CSF leakage was observed around the catheter. However, a 2–3 mm spread of CSF into the catheter was observed after withdrawal of the guiding needle, which corresponds to an estimated volume of 0.8–1.2  $\mu$ l. The head-up test was positive in all animals, confirming correct sacral catheter position within the subdural space. Before installation in the stereotaxic frame, CSF pressure values were not significantly different between the sham-operated group ( $4.8 \pm 0.4$  mmHg) and the SCI group ( $5.2 \pm 0.5$  mmHg) (Fig. 4). Neither were baseline values after installation significantly different between the sham-operated group ( $6.1 \pm 0.6$  mmHg) and the SCI group ( $6.6 \pm 0.5$  mmHg). CSF pressure was significantly higher in the SCI group ( $p < 0.0001$ ); at  $t_{60}$ , the values were  $5.5 \pm 0.5$  mmHg in the sham-operated group versus  $8.6 \pm 0.4$  mmHg in the SCI group. The CSF pressure increase after SCI was very steep between  $t_0$  and  $t_5$ , after which the value plateaued until  $t_{60}$ .

### Mean arterial blood pressure (MABP)

Baseline MABP was similar in the sham-operated group ( $111 \pm 4$  mmHg) and SCI group ( $115 \pm 5$  mmHg). Subsequently, MABP was significantly lower in the SCI group ( $p = 0.0396$ ): the values at  $t_{20}$  were  $114 \pm 5.6$  mmHg in the sham-operated group versus  $94 \pm 4$  mmHg in the SCI group and the values at  $t_{60}$  value were  $109 \pm 5$  mmHg in the sham-operated group versus  $95 \pm 3$  mmHg in the SCI group (Fig. 5).

### Spinal cord blood flow

We found no significant difference in baseline values between the sham-operated and SCI groups. SCBF values

showed no significant differences between the rostral and caudal probes, and we, therefore, pooled the values from the two probes. SCBF was significantly lower in the SCI group ( $p < 0.0001$ ) (Fig. 6). After SCI, the largest SCBF drop occurred from  $t_0$  to  $t_{20}$  and the decrease at  $t_{60}$  versus baseline was  $-63 \pm 4$  %.

### Integrity of the dura mater after SCI

The dura mater was intact in all animals, with no evidence of contrast-agent leakage on the myelographies ( $n = 5$ ) or of methylene-blue leakage by binocular inspection ( $n = 5$ ).

### Discussion

Our rat model allowed simultaneous measurement of CSF pressure and SCBF before and after a weight-dropping SCI that preserved dural integrity. We found that CSF pressure increased significantly within the first few hours after SCI, whereas SCBF decreased significantly around the epicentre.

After SCI, ischaemia is a major contributor to the secondary injury that worsens the initial cord lesions and, therefore, the neurological outcomes. The pathophysiology of ischaemia is complex, as it involves many different factors such as direct destruction of the micro-vasculature [23], systemic hypotension [4, 24], arterial vasospasm [25] and loss of cord autoregulation [26]. In analogy with brain perfusion, it has been suggested that the relationship between spinal cord perfusion, CSF pressure, and MABP can be assessed by computing spinal cord perfusion pressure (SCPP) as follows:  $SCPP = MABP - CSF$  pressure. This equation allows to understand why an increase in CSF pressure or a decrease in MABP can aggravate the spinal

**Fig. 5** Changes in mean arterial blood pressure (MABP) in the sham-operated and spinal cord injury (SCI) groups. Experimental SCI induced a significant decrease in MABP. The values shown correspond to mean  $\pm$  SEM

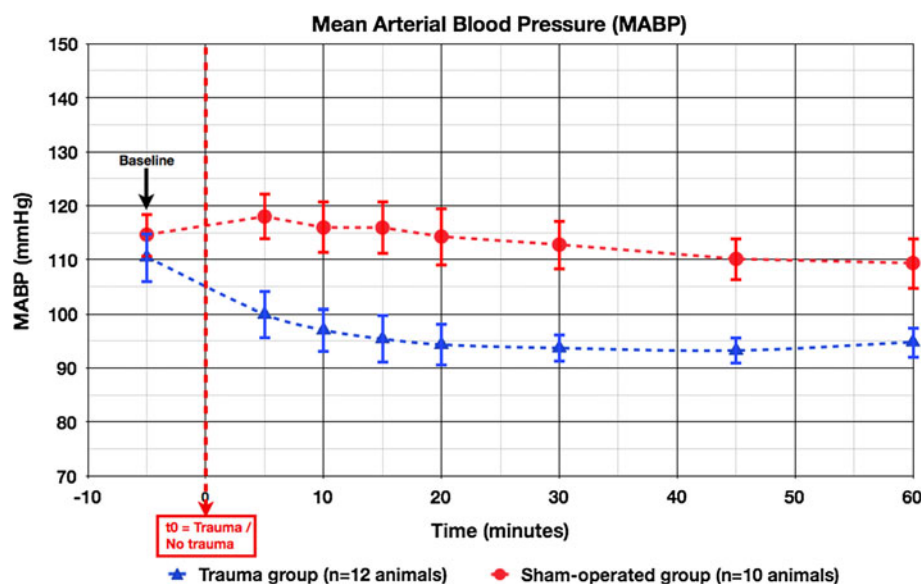
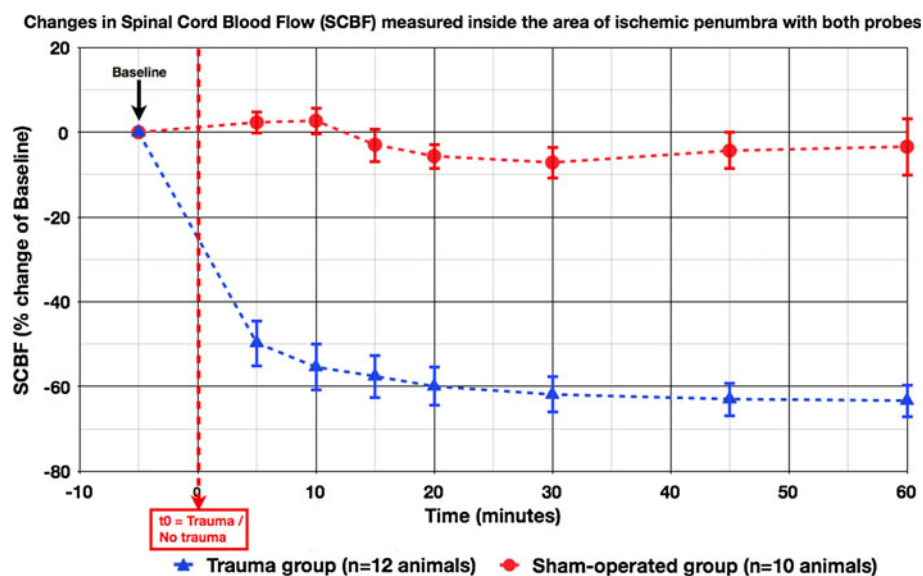


**Fig. 6** Changes in spinal cord blood flow (SCBF) measured using both laser-Doppler probes within the ischaemic penumbra zone surrounding the epicentre. As no significant difference was found between the rostral and caudal probes, the graph for each group corresponds to the average of the measurements of both probes. The values shown correspond to mean  $\pm$  SEM



cord ischaemia. As the dura is a watertight sac containing the CSF and the spinal cord, the effect of CSF pressure elevation on SCBF is usually ascribed to a tamponade effect on the small vessels of the cord. That suggests the concept of intradural compartment syndrome in analogy with leg compartment syndrome [27]. Two different clinical conditions can generate a decrease in SCBF, namely SCI and aorta cross clamping [5]. During surgical aortic cross-clamping, there is an arterial hypotension below the clamp inducing a significant decrease in SCBF at the thoracolumbar levels [28]. Meantime, there is an hypertension above the clamp, especially in the cerebral vasculature. Consequently, it elevates intracranial pressure, causes an increase in central venous pressure, and eventually leads to an increase in CSF pressure that aggravates the decline of SCBF as explained above [29]. In SCI, pathophysiology of

CSF elevation is different from aortic cross-clamping as there is no cerebral hypertension but rather a decrease in MABP due to the neurogenic shock [30] as we found in the present study. After SCI, elevation in CSF pressure is more ascribable to the increase of volume of the spinal cord due to the oedema and parenchymal haemorrhage. In further study, it will be of interest to use our model to assess the relationships between CSF, MABP and SCBF by varying MABP. In a canine model of thoracic aortic occlusion, the degree of spinal cord ischaemia was positively related to CSF pressure [18]. Moreover, CSF drainage during aorta cross-clamping significantly improves SCBF and is now considered an important method to decrease the rate of postoperative paraplegia due to spinal cord ischaemia [9, 17]. In acute SCI, the potential implication of CSF pressure in the pathophysiology has been emphasised by a recent

clinical trial which have shown that in patients with acute SCI, CSF pressure increased significantly during the decompressive surgery and in the postoperative period, reaching levels far above the physiological range [10]. A reasonable hypothesis is that maintaining CSF pressure within the normal range after SCI by drainage will decrease ischaemia severity, thereby improving neurological outcomes. To date, however, the potential benefits of CSF drainage on SCBF after SCI have not been studied. However, two studies suggest the relevance of that hypothesis. In rabbits, early CSF drainage via a lumbar catheter after SCI decreased the size of the histological cord lesions [20]. In rats subjected to mild spinal cord contusion, subdural space decompression by durotomy plus dural allografting was associated with improved neurological outcomes and with decreased cavitation and scar formation [31].

We have found no significant difference between rostral and caudal SCBF after SCI, which is consistent with the findings of Rivling and Tator [32] who used C14 autoradiographies to measure regional SCBF in rats. Reduction in regional SCBF is a consequence of parenchymal haemorrhage, and microvascular lesions which extent from the epicenter have been previously found to be similar in the rostral and caudal directions [4, 23], similar to the extent of ischaemia. We have chosen to position the probes very close to the epicenter in the so-called “penumbra zone” where the blood flow is significantly decreased and may evolve toward either improvement or degradation. Our model allows to measure SCBF in areas more remote from the epicenter but the penumbra zone is a region of major interest as all therapies tending to improve posttraumatic SCBF are targeted on it.

Macroscopically, the rat dura mater is thin and translucent. The dura mater of mammals is composed of longitudinal layers of collagen and elastin fibres, an architecture that results in limited circumferential tensile strength and stiffness [33–36]. Therefore, a weight-dropping trauma or catheter insertion might be expected to dissociate the collagen fibres, creating tears with CSF leakage. However, in our study, the use of a simple rounded and polished impactor similar to other marketed impactors did not induce dural tears. Moreover, to prevent CSF leakage around the catheters, we applied biological glue designed to serve as a sealant agent for dural tear repair [37]. Note that in the present study, no CSF leakage was observed between catheter insertion and application of glue. Several recent studies have emphasised the importance of incorporating the CSF layer into experimental models of SCI, as it plays an important biomechanical role in transmitting forces to the spinal cord [38, 39].

The values of physiological spinal CSF pressure that we found in rats lying in prone position, ranging from 4.8 to 5.2 mmHg were similar to those found in other studies.

Barth et al. [40] measured the cranial CSF pressure in rats and found a mean value of 5.6 mmHg. In another study, Budgell et al. [41] found a mean lumbar CSF pressure of 4.18 mmHg. In our study, we have found that when moving the head upward the sacral CSF pressure was immediately increased which is consistent with the literature. Indeed, Carlson et al. [42] and Klarica et al. [43] have demonstrated in dogs and cats, respectively, that when the head was elevated, the spinal CSF pressure was increased. CSF fills the entire dural sac from the skull to the sacrum and can be likened to a fluid column in which changes in pressures obey the laws of hydrodynamics. When the head is elevated, the hydrostatic height of this column increases and, therefore, the pressure measured at the lowest point, namely the sacrum, increases [6, 43]. For the same reason, elevation of the rat upon positioning in the stereotaxic frame induced an increase in CSF pressure measured at the sacrum.

One limitation of our study is the short duration of the experiment (1 h). In the above-mentioned clinical trial [10], the CSF pressure at the insertion of the catheter (acute phase) was about 14 mmHg and increased progressively with an intraoperative mean peak of 21.7 mmHg. In the no-drainage group, CSF pressure continued to increase until a mean peak of about 31 mmHg occurring 24 to 72 h after surgery. The increase of CSF pressure in the intact dura is due to the increase of volume of the spinal cord due to parenchymal haemorrhage and oedema [4]. Haemorrhage starts immediately after the trauma and stops precocely, conversely to oedema which course is slower [4]. We studied only the first hour after SCI and, therefore, did not obtain data on an important part of the course of CSF pressure. Given the duration of our experiment, our findings chiefly reflect the impact of bleeding on CSF pressure. However, our main objective was to assess the feasibility of measuring CSF pressure concomitantly with SCBF. Our results indicate no technical barriers to obtaining data on both variables over longer periods. Moreover, we plan to improve the model by inserting a second catheter for experimentally increasing the CSF pressure values, in order to reach higher values in less time. In the present study, no CSF leak was noted around the catheter when it was inserted and we have only observed a discrete spread of CSF into the catheter, where the volume was estimated to be about  $1\text{--}1.5\ \mu\text{l}$  ( $2\text{--}3\ \text{mm} \times \pi \times (0.4\ \text{mm} (24\text{G}))^2$ ). As the rate of CSF formation in the rat is about  $3\text{--}3.5\ \mu\text{l}/\text{min}$  [44], it is likely that the technique of catheter insertion had a negligible effect on the measured CSF pressure during the 60 min of the experiment.

Another limitation of our study is the smaller size of the rat subdural space compared to humans. To circumvent this anatomical limitation, other experimental studies have used bigger animals such as cats [45] or Yucatan miniature pigs [46, 47]. Compared to rats, bigger animals like pigs offer



the major advantage to have a ratio between volumes of spinal cord and subarachnoid space very similar to humans. Moreover, the more important size of the subarachnoid space in pigs makes possible the insertion of pressure transducers close to the epicenter of the injury while in rats, the lumbar cisterna is the only option caudal to the injury. However, despite the high relevance of models based on bigger animals and the necessity to use them to extrapolate experimental findings to humans, several arguments lead us to think that the rat also represents a valuable option for preliminary studies. First, it is the most used animal for experimental studies on SCI [19]. Second, it is cheaper, more accessible and requires less complex logistics for experiments, allowing for a decrease in cost and increase in sample size of preliminary studies. Third, the basal values of CSF pressure that we found in the rat (in horizontal position) as well as those reported in the literature range from 4 to 7 mmHg [40, 41, 48] which is close to the values reported in cats [20], pigs [46] and humans [6].

After SCI, it was shown in human [10] and in experimental settings [47] that a differential in CSF pressure across the injury site may occur. This emphasises the need for measuring CSF pressure caudal and rostral to the lesion. In our study, we only measured the CSF pressure caudal to the lesion but in rat, it is also possible to measure CSF pressure rostral to the injury level: Barth et al. [40] have proposed a technique to measure CSF pressure in the cisterna magna by inserting a catheter through the atlanto-occipital membrane, whereas Kusaka et al. [48] have simultaneously measured intracranial and spinal CSF pressure. In our study, the Th10 level of the experimental SCI does not preclude the surgical approach of the atlanto-occipital membrane and the relevance of the present model should be strongly improved by including the measurement of the CSF pressure rostral to the lesion.

## Conclusion

With the rat model described here, weight-dropping SCI can be induced without causing dural tears, and both CSF pressure and SCBF can be recorded continuously. We plan to use our model to investigate the effects of CSF drainage at the acute phase of SCI as a means of minimising spinal cord ischaemia.

**Conflict of interest** None.

## References

- Cadotte DW, Fehlings MG (2011) Spinal cord injury: a systematic review of current treatment options. *Clin Orthop Relat Res* 469:732–741. doi:10.1007/s11999-010-1674-0
- McDonald JW, Sadowsky C (2002) Spinal-cord injury. *Lancet* 359:417–425. doi:10.1016/S0140-6736(02)07603-1
- Beattie MS, Farrowqui AA, Bresnahan JC (2000) Review of current evidence for apoptosis after spinal cord injury. *J Neurotrauma* 17:915–925
- Mautes AE, Weinzierl MR, Donovan F, Noble LJ (2000) Vascular events after spinal cord injury: contribution to secondary pathogenesis. *Phys Ther* 80:673–687
- Martirosyan NL, Feuerstein JS, Theodore N, Cavalcanti DD, Spetzler RF, Preul MC (2011) Blood supply and vascular reactivity of the spinal cord under normal and pathological conditions. *J Neurosurg Spine* 15:238–251. doi:10.3171/2011.4.SPINE10543
- Fedorow CA, Moon MC, Mutch WA, Grocott HP (2010) Lumbar cerebrospinal fluid drainage for thoracoabdominal aortic surgery: rationale and practical considerations for management. *Anesth Analg* 111:46–58. doi:10.1213/ANE.0b013e3181d444d6
- Estrera AL, Sheinbaum R, Miller CC, Azizzadeh A, Walkes JC, Lee TY, Kaiser L, Safi HJ (2009) Cerebrospinal fluid drainage during thoracic aortic repair: safety and current management. *Ann Thorac Surg* 88:9–15. doi:10.1016/j.athoracsur.2009.03.039 (discussion 15)
- Coselli JS, Lemaire SA, Koksoy C, Schmittling ZC, Curling PE (2002) Cerebrospinal fluid drainage reduces paraplegia after thoracoabdominal aortic aneurysm repair: results of a randomized clinical trial. *J Vasc Surg* 35:631–639 pii:S0741521402791477
- Griep RB, Griep EB (2007) Spinal cord perfusion and protection during descending thoracic and thoracoabdominal aortic surgery: the collateral network concept. *Ann Thorac Surg* 83:S865–S869. doi:10.1016/j.athoracsur.2006.10.092 (discussion S890–S892)
- Kwon BK, Curt A, Belanger LM, Bernardo A, Chan D, Markez JA, Gorelik S, Slobogean GP, Umedaly H, Giffin M, Nikolakis MA, Street J, Boyd MC, Paquette S, Fisher CG, Dvorak MF (2009) Intrathecal pressure monitoring and cerebrospinal fluid drainage in acute spinal cord injury: a prospective randomized trial. *J Neurosurg Spine* 10:181–193. doi:10.3171/2008.10.SPINE08217
- Keenen TL, Antony J, Benson DR (1990) Dural tears associated with lumbar burst fractures. *J Orthop Trauma* 4:243–245
- Hamamoto Y, Ogata T, Morino T, Hino M, Yamamoto H (2007) Real-time direct measurement of spinal cord blood flow at the site of compression: relationship between blood flow recovery and motor deficiency in spinal cord injury. *Spine* 32:1955–1962. doi:10.1097/BRS.0b013e3181316310
- Tang Y, Shen HY, Huang L, Wu YF, Yang W, Ma YC, Yang R, Li J, Wang P (2008) Effect of intrathecal papaverine on blood flow and secondary injury in injured cord. *Spinal Cord* 46:716–721. doi:10.1038/sc.2008.30
- Guha A, Tator CH, Smith CR, Piper I (1989) Improvement in post-traumatic spinal cord blood flow with a combination of a calcium channel blocker and a vasopressor. *J Trauma* 29:1440–1447
- Westergren H, Farooque M, Olsson Y, Holtz A (2001) Spinal cord blood flow changes following systemic hypothermia and spinal cord compression injury: an experimental study in the rat using Laser-Doppler flowmetry. *Spinal Cord* 39:74–84
- Kato S, Kawahara N, Tomita K, Murakami H, Demura S, Fujimaki Y (2008) Effects on spinal cord blood flow and neurologic function secondary to interruption of bilateral segmental arteries which supply the artery of Adamkiewicz: an experimental study using a dog model. *Spine* 33:1533–1541. doi:10.1097/BRS.0b013e318178e5af (Phila Pa 1976)
- Bower TC, Murray MJ, Głowiczki P, Yaksh TL, Hollier LH, Pairello PC (1989) Effects of thoracic aortic occlusion and cerebrospinal fluid drainage on regional spinal cord blood flow in

- dogs: correlation with neurologic outcome. *J Vasc Surg* 9:135–144 pii:0741-5214(89)90228-0
18. Dasmahapatra HK, Coles JG, Wilson GJ, Sherret H, Adler S, Williams WG, Trusler GA (1988) Relationship between cerebrospinal fluid dynamics and reversible spinal cord ischemia during experimental thoracic aortic occlusion. *J Thorac Cardiovasc Surg* 95:920–923
  19. Young W (2002) Spinal cord contusion models. *Prog Brain Res* 137:231–255
  20. Horn EM, Theodore N, Assina R, Spetzler RF, Sonntag VK, Preul MC (2008) The effects of intrathecal hypotension on tissue perfusion and pathophysiological outcome after acute spinal cord injury. *Neurosurg Focus* 25:E12. doi:10.3171/FOC.2008.25.11.E12
  21. Shen XF, Zhao Y, Zhang YK, Jia LY, Ju G (2009) A modified ferric tannate method for visualizing a blood vessel and its usage in the study of spinal cord injury. *Spinal Cord*. doi:10.1038/sc.2009.30
  22. Soubeyrand M, Laemmel E, Dubory A, Vicaut E, Court C, Duranteau J (2012) Real-time and spatial quantification using contrast-enhanced ultrasonography of spinal cord perfusion during experimental spinal cord injury. *Spine* 37:E1376–E1382. doi:10.1097/BRS.0b013e318269790f (Phila Pa 1976)
  23. Koyanagi I, Tator CH, Lea PJ (1993) Three-dimensional analysis of the vascular system in the rat spinal cord with scanning electron microscopy of vascular corrosion casts. Part 2: Acute spinal cord injury. *Neurosurgery* 33:285–291
  24. Dolan EJ, Tator CH (1980) The treatment of hypotension due to acute experimental spinal cord compression injury. *Surg Neurol* 13:380–384
  25. Anthes DL, Theriault E, Tator CH (1996) Ultrastructural evidence for arteriolar vasospasm after spinal cord trauma. *Neurosurgery* 39:804–814
  26. Hickey R, Albin MS, Bunegin L, Gelineau J (1986) Autoregulation of spinal cord blood flow: is the cord a microcosm of the brain? *Stroke* 17:1183–1189
  27. Menetrey J, Peter R (1998) Acute compartment syndrome in the post-traumatic leg. *Rev Chir Orthop Reparatrice Appar Mot* 84:272–280 pii:MDOI-RCO-05-1998-84-3-0035-1040-101019-ART68
  28. Gharagozloo F, Neville RF Jr, Cox JL (1998) Spinal cord protection during surgical procedures on the descending thoracic and thoracoabdominal aorta: a critical overview. *Semin Thorac Cardiovasc Surg* 10:73–86 pii:S1043067998000112
  29. D'Ambra MN, Dewhirst W, Jacobs M, Bergus B, Borges L, Hilgenberg A (1988) Cross-clamping the thoracic aorta. Effect on intracranial pressure. *Circulation* 78:198–202
  30. Casha S, Christie S (2011) A systematic review of intensive cardiopulmonary management after spinal cord injury. *J Neurotrauma* 28:1479–1495. doi:10.1089/neu.2009.1156
  31. Smith JS, Anderson R, Pham T, Bhatia N, Steward O, Gupta R (2010) Role of early surgical decompression of the intradural space after cervical spinal cord injury in an animal model. *J Bone Joint Surg Am* 92:1206–1214. doi:10.2106/JBJS.I.00740
  32. Rivlin AS, Tator CH (1978) Regional spinal cord blood flow in rats after severe cord trauma. *J Neurosurg* 49:844–853. doi:10.3171/jns.1978.49.6.0844
  33. Runza M, Pietrabissa R, Mantero S, Albani A, Quaglini V, Contro R (1999) Lumbar dura mater biomechanics: experimental characterization and scanning electron microscopy observations. *Anesth Analg* 88:1317–1321
  34. Persson C, Evans S, Marsh R, Summers JL, Hall RM (2010) Poisson's ratio and strain rate dependency of the constitutive behavior of spinal dura mater. *Ann Biomed Eng* 38:975–983. doi:10.1007/s10439-010-9924-6
  35. Maikos JT, Elias RA, Shreiber DI (2008) Mechanical properties of dura mater from the rat brain and spinal cord. *J Neurotrauma* 25:38–51. doi:10.1089/neu.2007.0348
  36. Patin DJ, Eckstein EC, Harum K, Pallares VS (1993) Anatomic and biomechanical properties of human lumbar dura mater. *Anesth Analg* 76:535–540
  37. Kumar A, Maartens NF, Kaye AH (2003) Evaluation of the use of BioGlue in neurosurgical procedures. *J Clin Neurosci* 10:661–664 pii:S0967586803001632
  38. Jones CF, Kroeker SG, Cripton PA, Hall RM (2008) The effect of cerebrospinal fluid on the biomechanics of spinal cord: an ex vivo bovine model using bovine and physical surrogate spinal cord. *Spine* 33:E580–E588. doi:10.1097/BRS.0b013e31817ecc57 (Phila Pa 1976)
  39. Jones CF, Kwon BK, Cripton PA (2012) Mechanical indicators of injury severity are decreased with increased thecal sac dimension in a bench-top model of contusion type spinal cord injury. *J Biomech* 45:1003–1010. doi:10.1016/j.jbiomech.2012.01.025
  40. Barth KN, Onesti ST, Krauss WE, Solomon RA (1992) A simple and reliable technique to monitor intracranial pressure in the rat: technical note. *Neurosurgery* 30:138–140
  41. Budgell BS, Bolton PS (2007) Cerebrospinal fluid pressure in the anesthetized rat. *J Manipulative Physiol Ther* 30:351–356. doi:10.1016/j.jmpt.2007.04.002
  42. Carlson GD, Oliff HS, Gorden C, Smith J, Anderson PA (2003) Cerebral spinal fluid pressure: effects of body position and lumbar subarachnoid drainage in a canine model. *Spine* 28:119–122. doi:10.1097/01.BRS.0000041578.08645.3B (Phila Pa 1976)
  43. Klarica M, Rados M, Draganic P, Erceg G, Oreskovic D, Marakovic J, Bulat M (2006) Effect of head position on cerebrospinal fluid pressure in cats: comparison with artificial model. *Croat Med J* 47:233–238
  44. Chodobski A, Szmydynger-Chodobska J, Epstein MH, Johanson CE (1995) The role of angiotensin II in the regulation of blood flow to choroid plexuses and cerebrospinal fluid formation in the rat. *J Cereb Blood Flow Metab* 15:143–151. doi:10.1038/jcbfm.1995.16
  45. Shapiro K, Shulman K, Marmarou A, Poll W (1977) Tissue pressure gradients in spinal cord injury. *Surg Neurol* 7:275–279
  46. Jones CF, Lee JH, Kwon BK, Cripton PA (2012) Development of a large-animal model to measure dynamic cerebrospinal fluid pressure during spinal cord injury: laboratory investigation. *J Neurosurg Spine* 16:624–635. doi:10.3171/2012.3.SPINE11970
  47. Jones CF, Newell RS, Lee JH, Cripton PA, Kwon BK (2012) The pressure distribution of cerebrospinal fluid responds to residual compression and decompression in an animal model of acute spinal cord injury. *Spine* 37:E1422–E1431. doi:10.1097/BRS.0b013e31826ba7cd (Phila Pa 1976)
  48. Kusaka G, Calvert JW, Smelley C, Nanda A, Zhang JH (2004) New lumbar method for monitoring cerebrospinal fluid pressure in rats. *J Neurosci Methods* 135:121–127. doi:10.1016/j.jneumeth.2003.12.013